THE JOURNAL OF BIOLOGICAL CHEMISTRY VOL. 285, NO. 35, pp. 27289–27301, August 27, 2010
Printed in the U.S.A.

Postendocytic Sorting of Constitutively Internalized Dopamine Transporter in Cell Lines and Dopaminergic Neurons*[S]

Received for publication, April 6, 2010, and in revised form, May 21, 2010 Published, JBC Papers in Press, June 15, 2010, DOI 10.1074/jbc.M110.131003

Jacob Eriksen[‡], Walden Emil Bjørn-Yoshimoto[‡], Trine Nygaard Jørgensen[‡], Amy Hauck Newman[§], and Ulrik Gether[‡1]

From the [‡]Molecular Neuropharmacology Group and Center for Pharmacogenomics, Department of Neuroscience and Pharmacology, Faculty of Health Sciences, Panum Institute, University of Copenhagen, DK-2200 Copenhagen, Denmark and [§]Medicinal Chemistry Section, Intramural Research Program, National Institute on Drug Abuse, Baltimore, Maryland 21224

The dopamine transporter (DAT) mediates reuptake of released dopamine and is the target for psychostimulants, such as cocaine and amphetamine. DAT undergoes marked constitutive endocytosis, but little is known about the fate and sorting of the endocytosed transporter. To study DAT sorting in cells lines, we fused the one-transmembrane segment protein Tac to DAT, thereby generating a transporter (TacDAT) with an extracellular antibody epitope suited for trafficking studies. TacDAT was functional and endocytosed constitutively in HEK293 cells. According to an ELISA-based assay, TacDAT intracellular accumulation was increased by the lysosomal protease inhibitor leupeptin and by monensin, an inhibitor of lysosomal degradation and recycling. Monensin also reduced TacDAT surface expression consistent with partial recycling. In both HEK293 cells and in the dopaminergic cell line 1Rb3An27, constitutively internalized TacDAT displayed primary co-localization with the late endosomal marker Rab7, less co-localization with the "short loop" recycling marker Rab4, and little co-localization with the marker of "long loop" recycling endosomes, Rab11. Removal by mutation of N-terminal ubiquitination sites did not affect this sorting pattern. The sorting pattern was distinct from a *bona fide* recycling membrane protein, the β_2-adrenergic receptor, that co-localized primarily with Rab11 and Rab4. Constitutively internalized wild type DAT probed with the fluorescently tagged cocaine analogue JHC 1-64, exhibited the same co-localization pattern as TacDAT in 1Rb3An27 cells and in cultured midbrain dopaminergic neurons. We conclude that DAT is constitutively internalized and sorted in a ubiquitination-independent manner to late endosomes/lysosomes and in part to a Rab4 positive short loop recycling pathway.

The dopamine transporter (DAT)[2] mediates reuptake of dopamine from the synaptic cleft and terminates in this way dopaminergic signaling and mediates recycling of released dopamine (1–3). Alteration in dopamine signaling and DAT function is coupled to neurological and psychiatric diseases including schizophrenia, bipolar disorder, attention deficit hyperactivity disorder, Tourette syndrome, and Parkinson disease (2, 4, 5). DAT is the principle target for widely abused psychostimulants, such as cocaine and amphetamine (1–3). The transporter belongs to the family of neurotransmitter-sodium symporters (also called the SLC6 (solute carrier 6) family or Na^+/Cl^--coupled transporters) that also includes the transporters for other neurotransmitters, such as the norepinephrine, serotonin, glycine, and γ-aminobutyric acid transporters. Neurotransmitter-sodium symporter proteins utilize the transmembrane Na^+ gradient as a driving force for transport of substrate and are further characterized by additional co-transport of Cl^- (2, 3, 6).

Numerous studies have supported that DAT is subject to dynamic regulation in the plasma membrane, thereby providing a means of attenuating or increasing the strength of dopaminergic signaling. The most intensively studied mechanism is the regulatory effect of protein kinase C (PKC) activation. It has been demonstrated in several DAT-transfected heterologous cell lines as well as in synaptosomes that activation of PKC by phorbol esters, such as phorbol 12-myristate 13-acetate (PMA), down-regulates dopamine transport (6–13). The sustained DAT down-regulation in response to PKC activation is believed mainly to be a result of DAT endocytosis through a clathrin-dependent mechanism (6, 7, 9, 10). In addition, DAT trafficking is regulated by other protein kinases, such as MAPK and Akt (14, 15), as well as by substrates and inhibitors (16).

DAT also undergoes a marked constitutive endocytosis, a property that first was described in heterologous cell lines (6, 10, 17). Subsequent mutational analyses suggested that this constitutive internalization is promoted by a non-conventional trafficking motif in the DAT C terminus (10, 18) and possibly negatively regulated by residues residing in the membrane-proximal DAT N terminus (19). Recently, we demonstrated by

* This work was supported, in whole or in part, by National Institutes of Health Grant P01 DA 12408 (to U. G.) and by the National Institute on Drug Abuse Intramural Research Program (to A. H. N.). This work was also supported by the Lundbeck Foundation (to U. G.), the Danish Medical Research Councils (to U. G.), and "Fabrikant Vilhelm Pedersen og Hustrus Mindelegat" (to U. G.).

[S] The on-line version of this article (available at http://www.jbc.org) contains supplemental Figs. S1–S3.

[1] To whom correspondence should be addressed: Dept. of Neuroscience and Pharmacology, Panum Inst. 18.6, Blegdamsvej 3, DK-2200 Copenhagen N, Denmark. Tel.: 45-35327548; Fax: 45-35327610; E-mail: gether@sund.ku.dk.

[2] The abbreviations used are: DAT, dopamine transporter; PMA, phorbol 12-myristate 13-acetate; EGFP, enhanced GFP; CFT, (−)-2-β-carbomethoxy-3-β-(4-fluorophenyl)tropane; ANOVA, analysis of variance; SERT, serotonin transporter; hDAT, human DAT; PKC, protein kinase C.

using the fluorescent cocaine analogue JHC 1-64 as label that DAT endogenously expressed in cultured midbrain dopaminergic neurons undergoes constitutive internalization (8). The constitutive DAT internalization was dynamin-dependent, and internalized transporter partially co-localized with the early endosomal marker Rab5 and with endocytosed transferrin (8).

A major question is the fate of the constitutively internalized transport protein. Previous studies in heterologous cells have indicated that DAT might be sorted to a recycling pathway (10, 17); however, postendocytic sorting of constitutively internalized DAT has not yet been analyzed in dopaminergic neurons, and postendocytic sorting of constitutively internalized DAT in heterologous cells has not been analyzed in dynamic imaging experiments using co-expressed markers of distinct endocytic compartments. In the present study, we investigated the postendocytic sorting of constitutively internalized DAT in both heterologous cells and cultured dopaminergic neurons. We took advantage of a fusion protein between the one-transmembrane segment protein Tac and DAT, which provides a transporter (TacDAT) with an extracellular N-terminal antibody epitope. In the absence of a DAT antibody directed toward an endogenous extracellular epitope, TacDAT enables the application of antibody feeding experiments and implementation of ELISA-based trafficking assays. Moreover, by use of the fluorescent cocaine analogue JHC 1-64, we are able to analyze postendocytic sorting of DAT in cultured dopaminergic neurons. Taken together, our data suggest that constitutively internalized DAT is sorted to a late endosomal/lysosomal degradative pathway as well as in part to a "short loop" recycling pathway in both neurons and cell lines.

EXPERIMENTAL PROCEDURES

Molecular Biology—TacDAT was generated by a two-step PCR procedure. First, FLAG-Tac was amplified from pcDNA3 FLAG-Tac (20) with primers generating an overhang identical to the N-terminal part of DAT. Second, DAT was amplified from a synthetic cDNA encoding the human DAT (synDAT) (21) in pcDNA3 with a 5′ overhang identical to the C-terminal part of FLAG-Tac. The products from the first round of PCR were used as template for generating a TacDAT fragment that subsequently was cloned into the pcDNA3 synDAT vector using KpnI and BamHI. The HA-DAT 3KR mutant in pcDNA3 was made by changing lysines 19, 27, and 35 to arginines in HA-DAT (8, 22) using QuikChange site-directed mutagenesis (Stratagene). The plasmid pcDNA3.1 FLAG-β_2-adrenergic receptor was a kind gift from Dr. Mark von Zastrow, University of California, San Francisco, CA; pJPA5 transferrin receptor-GFP was a kind gift from Dr. Bo van Deurs, University of Copenhagen, Copenhagen, Denmark; and pEGFP-Rab4 was a kind gift from Dr. José A. Esteban, Universidad Autónoma de Madrid, Madrid, Spain. The plasmids pEGFP-Rab7 and pEGFP-Rab11 were kind gifts from Dr. Katherine W. Roche, National Institute of Neurological Disorders and Stroke, Bethesda, MD. The plasmids pHsSynXW enhanced GFP (EGFP)-Rab7 and -Rab11 were generated by PCR, amplifying the cDNA encoding region EGFP-Rab7 and -Rab11 from pEGFP-Rab7 and pEGFP-Rab11, respectively. After digestion with BsiWI + MluI, fragments were ligated into the lentiviral transfer vector pHSynCXW (8). EGFP-Rab4 was cloned into pHsSynXW by excising EGFP-Rab4 from pEGFP-Rab4 with NheI and SalI and ligated into pHsSynXW digested with SpeI and SalI. The sequences of the cDNAs were verified by sequencing.

Cell Cultures and Lentivirus Production—HEK293 cells and 1Rb3An27 cells were grown in DMEM with 10% FCS and transfected using standard Lipofectamine 2000 protocols (Invitrogen) 2 days prior to the experiment. Postnatally derived rat midbrain dopaminergic neurons were prepared as described previously (8) using a protocol modified from that of Rayport *et al.* (23). Briefly, the cultures were obtained from the ventral midbrain of 1–3-day-old pups. The dissected tissue sample was digested in a papain solution for 30 min at 37 °C while slowly superfusing with a mixture of 95% O_2 and 5% CO_2. The digested tissue was carefully triturated into single cells using increasingly smaller pipette tips. The cells were centrifuged at 500 × *g* for 5 min and resuspended in warm SF1C consisting of 50% modified Eagle's medium, 40% DMEM, and 10% Ham's F-12 nutrient mixture (all from Invitrogen) supplemented with 2.5 mg/ml bovine serum albumin, 0.35% D-glucose, 0.5 mM glutamine, 1% heat-inactivated calf serum (Invitrogen), 5 mM kynurenic acid, 12 units/ml penicillin, 12 μg/ml streptomycin, 0.05% liquid catalase, and diPorzio (24). The neurons were plated on a monolayer of glial cells grown in Lab-Tek wells (Nunc). The cells were allowed to settle for ~2 h before addition of glial cell line-derived neurotrophic factor (Millipore Bioscience Research Reagents) (10 ng/ml). The next day 5-fluorodeoxyuridine was added to inhibit growth of glial cells.

Lentiviral vectors were produced as described previously (8) according to procedures modified from Naldini *et al.* (25). HEK293T packaging cells were transiently triple transfected with the following: 1) packaging plasmid encoding viral structure proteins (pBRΔ8.91), 2) envelope plasmid encoding the envelope protein vesicular stomatitis virus glycoprotein (pMD.G), and 3) transfer plasmid containing the gene of interest (pHsSynXW EGFP-Rab4, -Rab7, or -Rab11). The transfections were performed in DMEM (Invitrogen) supplemented with 10% FBS (Invitrogen) using calcium phosphate precipitation. Medium was replaced with fresh medium after 5 h. Approximately 48 and 72 h after transfection, media containing lentivirus were collected, centrifuged, filtered, and concentrated by ultracentrifugation at 50,000 × *g* for 1.5 h at 4 °C. The virus-containing pellet was resuspended in modified Eagle's medium (Sigma) at ½80 of the original volume and stored in aliquots at −80 °C. The neuronal cultures were incubated with concentrated lentivirus on days 2–3 *in vitro*, and experiments were performed 8–12 days after infection.

[^{3}H]Dopamine Uptake Experiments—Uptake assays were carried out as described previously (21) using 2,5,6-[^{3}H]dopamine (30–60 Ci/mmol, PerkinElmer Life Sciences) and HEK293 cells transfected with equal amounts of pcDNA3 synDAT or pcDNA3 TacDAT plated in 24-well plates (10^5 cells/well). The uptake assays were carried out 2 days after transfection for 3 min at room temperature (20–22 °C) in uptake buffer (25 mM HEPES, 130 mM NaCl, 5.4 mM KCl, 1.2 mM $CaCl_2$, 1.2 mM $MgSO_4$, 1 mM L-ascorbic acid, 5 mM D-glucose, and 1 M catechol-*O*-methyltransferase inhibitor Ro 41-0960 (Sigma), pH

7.4). A serial dilution of non-labeled dopamine, cocaine, or nomifensine was added to the cells prior to initiation of uptake with ~10 nM [^{3}H]dopamine.

[N-methyl-^{3}H](−)-2-β-Carbomethoxy-3-β-(4-fluorophenyl)tropane ([^{3}H]CFT) Binding Experiments—Binding experiments were carried out using [^{3}H]CFT (76 Ci/mmol; PerkinElmer Life Sciences) essentially as described (26). Briefly, HEK293 cells transiently transfected with equal amounts of pcDNA3 synDAT or pcDNA3 TacDAT were plated in 24-well plates (10^5 cells/well) 1 day after transfection, and the binding experiment was carried out 2 days after transfection. A serial dilution of non-labeled CFT was added to the cells prior to addition of 3 nM [^{3}H]CFT and incubation for 60 min at 4 °C in uptake buffer.

ELISA Internalization Assay—HEK293 cells were transfected with pcDNA3 Tac or pcDNA3 TacDAT using Lipofectamine 2000 (Invitrogen) at a 1:3 ratio to obtain similar surface expression and seeded in 96-well plates (35,000 cells/well) the next day. The experiment was performed 2 days after transfection. First, the cells were incubated with M1 (1 μg/ml) in DMEM for 30 min at 4 °C, and then medium was replaced with 37 °C DMEM and placed at 37 °C (or 4 °C for surface quantification) for various periods with different compounds to drive internalization. To strip off surface M1, the cells were incubated with an acid strip buffer (0.5 M NaCl and 0.2 M acetic acid) for 5 min on ice, then washed twice with phosphate-buffered saline (PBS), fixed in 4% paraformaldehyde in PBS, and again washed twice in PBS. The cells were then blocked and permeabilized in PBS with 5% goat serum and 0.05% Triton X-100 for 30 min (background subtraction was done with cells that were not permeabilized). Then the cells were incubated with horseradish peroxidase-conjugated goat antimouse antibody (1:1000; Pierce) in PBS + 5% goat serum for 30 min and washed two times in blocking buffer and two times in PBS. SuperSignal ELISA Femto Maximum Sensitivity Substrate (Pierce) was added to the wells, and the luminescence was detected in a Wallac Victor2 plate reader after 2 min.

Surface ELISA—HEK293 cells, transfected with plasmids encoding HA-hDAT, TacDAT, FLAG-β_2-adrenergic receptor, or transferrin receptor-GFP, were seeded in 96-well plates (35,000 cells/well) the day before the experiment. On the day of the experiment, the cells were incubated with monensin (25 μM) or vehicle for 1 h at 37 °C. Next, the cells were fixed in 4% paraformaldehyde in PBS for 20 min on ice; washed twice in PBS; blocked in PBS + 5% goat serum for 30 min; and incubated with M1 (1:5000) for TacDAT and FLAG-β_2-adrenergic receptor, HA.11 antibody (1:1000; Covance, Princeton, NJ) for HA-DAT, and anti-GFP for GFP-transferrin receptor (1:2000) in PBS + 5% goat serum for 60 min. Following four washes in PBS, the cells were then incubated with horseradish peroxidase-conjugated goat anti-mouse antibody against M1 and HA.11 or horseradish peroxidase-conjugated goat anti-rabbit antibody against anti-GFP for 30 min and subsequently washed four additional times in PBS. The horseradish peroxidase activity was measured as described above.

Immunofluorescence Antibody Internalization Assays—HEK293 cells or 1Rb27An3 cells were transfected with Lipofectamine 2000 2 days prior to the experiment and seeded on coverslips treated with polyornithine the next day. The cells were incubated with M1 antibody (1 μg/ml) in DMEM for 30 min at 4 °C. The medium was then replaced with 37 °C DMEM and placed at 37 °C for various periods to drive internalization. The internalization was stopped by washing with cold PBS followed by fixation in 4% paraformaldehyde in PBS, and cells were washed three times in PBS and permeabilized in PBS with 5% goat serum and 0.2% saponin. Alexa Fluor 568 anti-mouse antibody (1:500; Molecular Probes) against M1 in PBS + 5% goat serum was added for 30 min, and then the specimens were washed three times in PBS prior to mounting.

For the co-localization experiments, cells were transfected with equal amounts of plasmid encoding TacDAT or FLAG-tagged β_2-adrenergic receptor and EGFP-Rab4, -Rab7, or -Rab11 and seeded on coverslips treated with polyornithine. On the day of the experiment, the cells were incubated with Alexa Fluor 568-conjugated M1 antibody for 30 min at 4 °C, and the medium was then replaced with 37 °C DMEM (+10 μM isoproterenol for experiments with the β_2-adrenergic receptor) and placed at 37 °C for 1 h to allow internalization. The cells were subsequently fixed in 4% paraformaldehyde in PBS and mounted. The stained cells were visualized using a Zeiss LSM 510 confocal laser-scanning microscope using an oil immersion numerical aperture 1.4 63× objective (Zeiss, Jena, Germany). EGFP was excited with the 488 nm laser line from an argon-krypton laser, and the emitted light was detected using a 505–550-nm band pass filter, whereas the Alexa Fluor 568 dye was excited at 543 nm with a helium-neon laser, and the emitted light was detected using a 585-nm long pass filter. The resulting images were combined using ImageJ[3] software.

Co-localization Quantification—Quantification of co-localization with EGFP-tagged Rab4, Rab7, and Rab11 was done using the RG2B co-localization plug-in to ImageJ[3] as described (20, 27). Single cells were defined as regions of interest to avoid noise from untransfected cells and nonspecific staining. A minimum threshold pixel intensity of 120 was set for each channel, and the minimum ratio for pixel intensity between the two channels was set to 0.5. Results are displayed as percent co-localization as determined by dividing the area of co-localization pixels by the total area over the threshold of the M1 signal. 30–35 cells were used for quantification under each condition. Statistical significance was determined using a one-way ANOVA with Bonferroni's multiple comparison test. Differences were considered significant when $p < 0.05$.

DAT Internalization with JHC 1-64—1Rb3An27 cells or dopaminergic neurons were grown in poly-L-ornithine-treated Lab-Tek chambers. On the day of the experiment, the cells were incubated with the rhodamine-conjugated fluorescent cocaine analogue JHC 1-64 (28) in uptake buffer for the designated time periods. To detect internalization in midbrain dopaminergic neurons and 1Rn27An3 cells, the cultures were incubated with 5 nM JHC 1-64 in uptake buffer for 30 min at 4 °C, the buffer was removed and replaced with 37 °C uptake buffer, and the cultures were incubated for 60 min at 37 °C. For the LysoTracker co-localization experiment, we used LysoTracker Green (100 nM; Molecular Probes) in the last 10 min of incubation, and

[3] W. S. Rasband (1997–2006) ImageJ, National Institutes of Health.

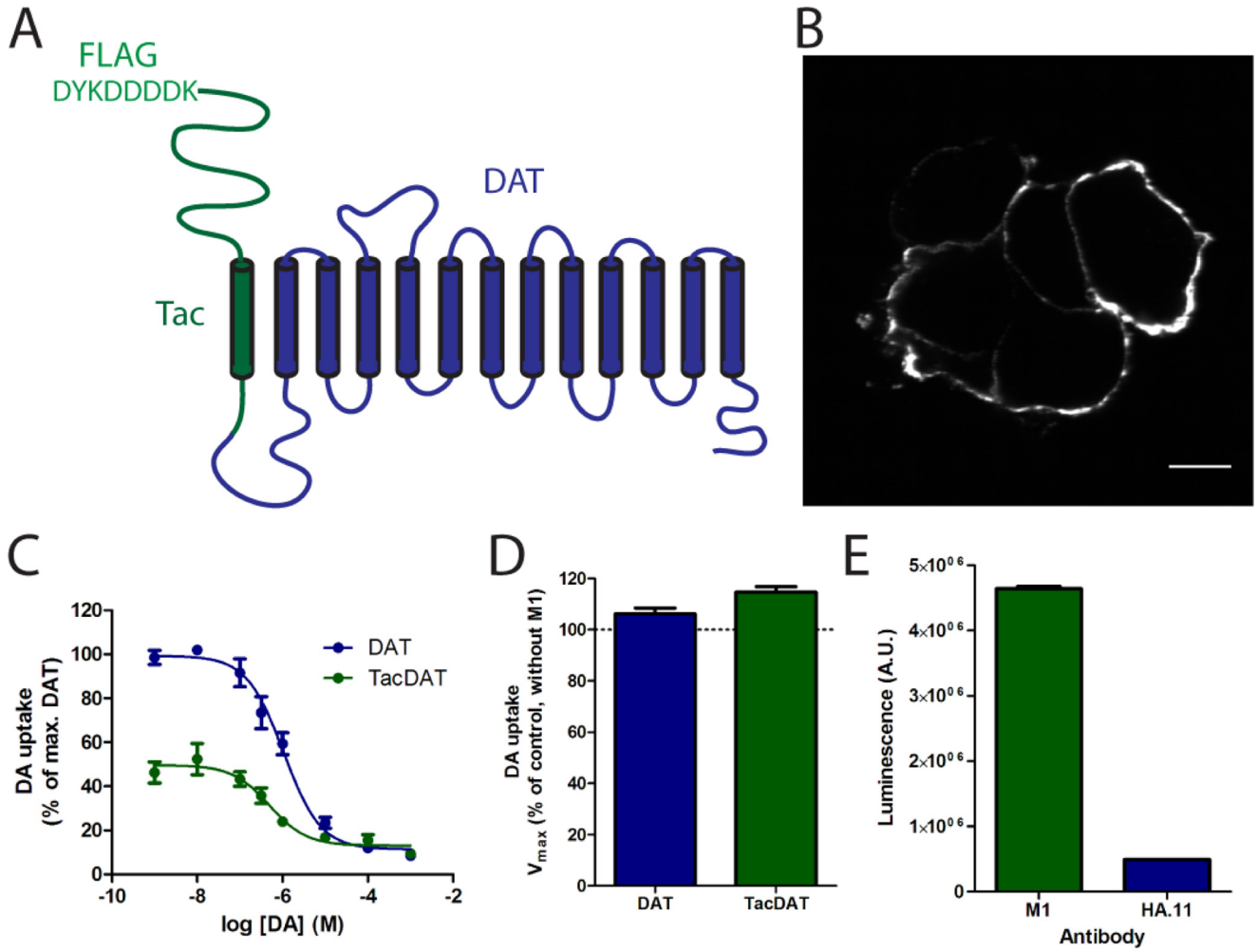

FIGURE 1. **Thirteen-transmembrane segment fusion protein between DAT and Tac contains high affinity FLAG epitope and is functionally expressed in plasma membrane of HEK293 cells.** *A*, TacDAT is a head-to-tail fusion of hDAT (*blue*) and Tac (*green*) with an N-terminal M1 antibody FLAG epitope, DYKDDDDK. *B*, non-permeabilizing immunostaining of HEK293 cells transfected with TacDAT using an M1 antibody recognizing the FLAG epitope. *Scale bar*, 10 μm. *C*, [^{3}H]dopamine (*DA*) uptake experiments in HEK293 cells transfected with TacDAT (*green*) or hDAT (*blue*). The data are shown as relative uptake in percentage of [^{3}H]dopamine uptake in wild type DAT (means ± S.E., $n = 3$ of triplicate determinations). *D*, [^{3}H]dopamine uptake after preincubating HEK293 cells expressing TacDAT or hDAT for 30 min at 4 °C with M1 antibody. Data are means ± S.E. of $n = 3$. *E*, surface HA.11 and M1 ELISA signals from HEK293 cells expressing TacDAT with an inserted HA tag in the second extracellular loop (Tac-HA-DAT). Values are means ± S.E. of $n = 3$. *A.U.*, arbitrary units.

subsequently the cells were washed in uptake buffer. After incubation, the living cells were imaged at room temperature using a Zeiss LSM 510 confocal laser-scanning microscope with a 63× numerical aperture 1.4 objective. JHC 1-64 was visualized using a 543 nm helium-neon laser line and a 585-nm long pass filter, EGFP was detected with a 488 nm argon-krypton laser line and a 505–550-nm band pass filter, and the distribution of JHC 1-64 on the neurons were analyzed with a Z-scan.

RESULTS

To enable the study of DAT trafficking with high specificity and to detect even small amounts of DAT endocytosis, we wanted to generate a DAT construct with a high affinity extracellular antibody epitope. Instead of disrupting the extracellular loops, we decided to add an extra transmembrane segment to the DAT N terminus. This was done by taking advantage of the single transmembrane segment protein Tac and making a "head-to-tail" fusion of the DAT and a Tac construct containing an M1 antibody FLAG epitope after the Tac signal sequence (20) (Fig. 1*A*). Note that Tac fusion proteins have been used previously as a "silent reporter" in several trafficking studies (18, 29–31).

The resulting construct, TacDAT, was expressed transiently in HEK293 cells, and immunostaining with the M1 monoclonal anti-FLAG antibody demonstrated in the absence of permeabilization a clear surface staining, confirming that the N-terminal antibody epitope is exposed on the extracellular side of the plasma membrane and that the protein is expressed at the cell surface (Fig. 1*B*). TacDAT was functionally analyzed in [^{3}H]dopamine uptake experiments in transiently transfected HEK293 cells (Fig. 1*C*). TacDAT mediated uptake with a K_m value of ~0.40 μM as compared with ~0.92 μM for DAT and displayed a partially reduced uptake capacity (Fig. 1*C* and Table 1). We also performed binding assays with the high affinity cocaine analogue [^{3}H]CFT, which showed an affinity for TacDAT of ~8 nM compared with ~19 nM for DAT and a partially reduced B_{max} (Table 1). The DAT inhibitors cocaine and nomifensine also showed a slightly higher apparent affinity (~2-fold increase) for

TABLE 1

Functional properties of TacDAT compared with DAT

All values are means (S.E. interval) for the K values and mean ± S.E. for V_{max} and B_{max} derived from three independent experiments performed in HEK293 cells. The K_m and K_d values were calculated from the pIC_{50} values determined by non-linear regression analysis of [^{3}H]dopamine uptake and [^{3}H]CFT binding data as described previously (12, 26). The S.E. intervals were calculated from pK ± S.E. The K_i values were calculated from IC_{50} values determined by non-linear regression analysis of uptake data and using the equation $K_i = IC_{50}/(1+ (L + K_m))$ where L is the concentration of [^{3}H]dopamine. The S.E. interval was calculated from pK ± S.E. All data calculations were done using Prism 5.0 from GraphPad Software, San Diego, CA.

	DAT	TacDAT
[^{3}H]Dopamine K_m (μM)	0.92 (0.62–1.4)	0.40 (0.36–0.47)
[^{3}H]Dopamine V_{max} (fmol/min/10^5)	2486 ± 236	511 ± 104
Cocaine K_i (nM)	154 (128–187)	86.4 (66.6–112)
Nomifensine K_i (nM)	75.1 (49.3–114)	45.7 (31.9–65.4)
[^{3}H]CFT K_d (nM)	18.8 (15.3–23.0)	8.32 (7.80–8.87)
[^{3}H]CFT B_{max} (nM)	217 ± 33	69.0 ± 8.0

TacDAT as compared with DAT. Taken together, the data show that TacDAT is functional with a pharmacology very similar to that of DAT. Because our experiments would involve TacDAT with M1 bound, we also made sure that binding of the M1 antibody to TacDAT did not affect transporter function as determined by measuring [^{3}H]dopamine uptake in the presence of bound M1 antibody (Fig. 1*D*).

Previously, an HA tag was successfully introduced into the second extracellular loop of DAT (22). We decided to compare this tag directly with the FLAG tag in TacDAT and generated a TacDAT construct harboring also the HA tag (Tac-HA-DAT). Because of potential differences in expression and thereby in the number of tagged transporters, such a direct comparison would only be possible in this construct with both tags present in the same protein. We tested the surface expression of Tac-HA-DAT by using a cell surface ELISA and using either M1 anti-FLAG antibody or HA.11 anti-HA antibody. Interestingly, the signal from the FLAG epitope was almost 10-fold higher than the corresponding signal from the HA epitope (Fig. 1*E*). This suggests that TacDAT might be advantageous for quantitative studies of DAT trafficking.

Next, we wanted to test whether it was possible to characterize previously proposed DAT trafficking properties using TacDAT in antibody-based internalization assays. HEK293 cells transfected with TacDAT or with Tac as a negative control were incubated with M1 antibody at 4 °C to label surface Tac or TacDAT. Subsequently, the cells were incubated at 37 °C to allow internalization for 30 min (Fig. 2*A*). After 30 min of internalization, a visible intracellular accumulation of TacDAT was seen, consistent with constitutive endocytosis as described previously for DAT (8, 10, 17) (Fig. 2*C*). No visible intracellular accumulation of Tac was observed (Fig. 2*B*). To further investigate the trafficking properties of TacDAT, we stimulated TacDAT-expressing HEK293 cells with PMA. Addition of PMA (1 μM) during the 30-min internalization period increased substantially the amount of intracellular localized TacDAT (Fig. 2*C*), suggesting that TacDAT is internalized in response to PMA as also observed for DAT in HEK293 cells (6, 8). Tac alone did not respond to PMA (data not shown).

Taken together, our data suggest that TacDAT not only is functional but also has retained the well described trafficking properties of DAT in HEK293 cells. We decided, therefore, to use TacDAT in our further investigations. The presence of the efficient extracellular FLAG epitope permitted the use of a quantitative ELISA-based internalization assay. To perform the assay, TacDAT- or Tac-expressing cells were labeled with M1 antibody at 4 °C before internalization was allowed for 5–60 min with or without addition of PMA or the substrate amphetamine. Surface antibody was removed by acid strip, and intracellular transporter was measured by ELISA upon permeabilization of cells (Fig. 2*D*). Internalization was calculated as the amount of intracellularly accumulated TacDAT relative to initial TacDAT surface expression. In HEK293 cells transiently expressing TacDAT, a time-dependent and saturating internalization was observed (Fig. 2*E*). Incubation with either amphetamine (10 μM) or PMA (1 μM) increased TacDAT internalization over time (Fig. 2*E*), whereas in cells transfected with Tac, no increase in the internalization was observed for PMA or amphetamine at any time point as compared with untreated Tac (Fig. 2*E*). The largest effects of the treatments were seen after 60 min of incubation (Fig. 2*F*) with a tendency toward saturation for all conditions (Fig. 2*E*).

We explored whether we could use the quantitative ELISA to investigate the fate of the constitutively internalized transporter (Fig. 2, *C* and *E*). Specifically, we attempted to assess whether the internalized TacDAT was sorted to either lysosomal degradation or recycling by using compounds blocking either lysosomal degradation (the protease inhibitor leupeptin) or both recycling and lysosomal degradation (the cation ionophore monensin) (32). Leupeptin (100 μg/ml, 1 h) increased significantly the accumulated M1 antibody signal in HEK293 cells transiently expressing TacDAT, whereas no significant effect was seen in cells transiently expressing Tac (Fig. 3*A*). An even more pronounced effect was observed for monensin (25 μM, 1 h) on the intracellular accumulation of TacDAT (Fig. 3*A*). This effect could be the result of either inhibited lysosomal degradation or inhibited recycling. If it was the result of blocking recycling, a concomitant decrease in surface expression would be expected during the same period. We tested this using the surface ELISA and observed a significant decrease in both TacDAT (88 ± 2.2% of vehicle) and HA-DAT surface expression (94 ± 0.2% of vehicle) upon monensin treatment (Fig. 3*B*). In parallel, we tested the effect of monensin on the surface expression of the well established recycling membrane proteins, the β_2-adrenergic receptor (33, 34) and the transferrin receptor (35). As expected, both the β_2-adrenergic receptor (76 ± 3.5% of isoproterenol-treated) and the transferrin receptor (79 ± 3.8% of vehicle) were affected by monensin and to a higher degree than for any of the DAT constructs (Fig. 3*B*). As a control, we tested the effect of monensin on non-agonist-treated and thereby non-internalized β_2-adrenergic receptor and found no significant effect of monensin (Fig. 3*B*). Altogether, the ELISA results suggest that constitutively internalized DAT in HEK293 cells is sorted both to lysosomal degradation and in part to a recycling pathway.

Rab proteins are small GTPases that organize membrane protein trafficking (36) and serve as markers of distinct endosomal compartments. To get further insight into DAT sorting, we used confocal imaging together with co-expression of

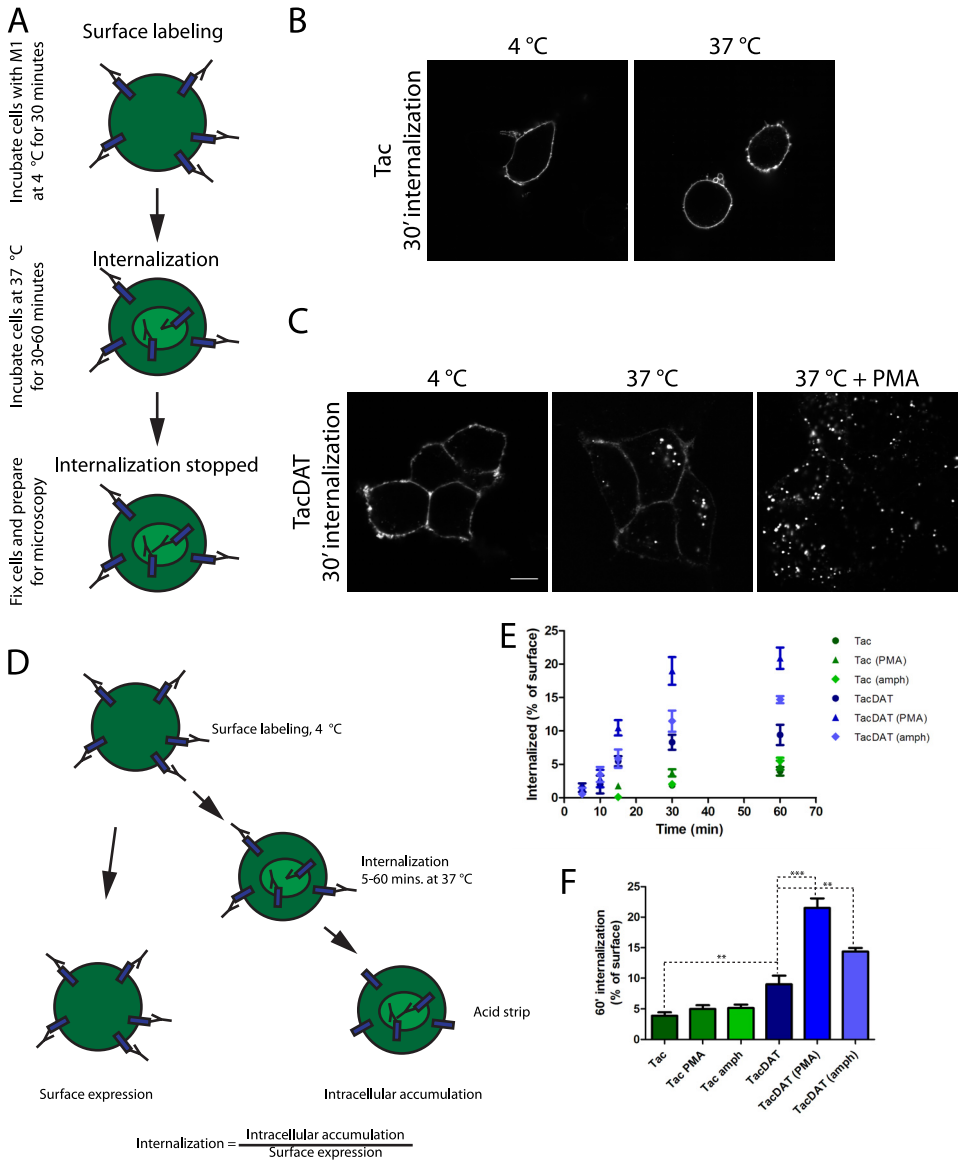

FIGURE 2. **Visualizing and quantifying TacDAT internalization using M1 antibody-based internalization assays.** *A*, to detect TacDAT internalization, we established a conventional antibody internalization assay in which we first labeled the cells with M1 antibody at 4 °C to label surface TacDAT at a temperature that blocked trafficking. Next, the cells were incubated at 37 °C in new medium for 30–60 min to allow internalization of TacDAT. For surface detection alone, the cells were kept at 4 °C. Subsequently, cells were fixed, permeabilized, and incubated with secondary fluorophore-conjugated antibody. The fluorescence was visualized using confocal microscopy. *B*, confocal images of HEK293 cells expressing Tac assayed as just described. *C*, the same assay with HEK293 cells expressing TacDAT. During the 30-min incubation at 37 °C, cells were incubated with or without the PKC activator PMA (1 μM). The images are representative of at least three similar experiments. *D*, brief description of ELISA-based internalization assay. As for the conventional microscopy-based internalization assay described above, cells were first labeled with M1 at 4 °C and then either incubated at 4 °C for surface detection or incubated at 37 °C for various periods to allow internalization. After the internalization period, the cells were placed on ice, and the surface antibody was stripped off using an acid strip buffer. After fixation, the cells were permeabilized, and the intracellular accumulated antibody was detected with a horseradish peroxidase-conjugated secondary antibody. The internalization signal was expressed as the proportion of the start surface signal. *E*, intracellular accumulation assessed by ELISA (as just described) in HEK293 cells transiently expressing TacDAT or Tac. Internalization was performed without or with PMA (1 μM) or amphetamine (10 μM) for the indicated times. Values are means ± S.E. of $n = 6$. *F*, intracellular accumulation after 60 min of internalization (means ± S.E. of $n = 6$; **, $p < 0.01$; ***, $p < 0.001$; one-way ANOVA with Bonferroni's multiple comparison test). *amph*, amphetamine; ′, minutes.

TacDAT and Rab proteins tagged with EGFP in HEK293 cells. This included EGFP-Rab4 to visualize early endosomes and the "short loop recycling" pathway, EGFP-Rab7 to visualize late endosomes, and EGFP-Rab11 to visualize recycling endosomes and the "long loop" recycling pathway (36, 37). The internalization assay was carried out with 1 h of internalization as described in Fig. 2*A* except that we used a primary fluorophore-conjugated M1 antibody. This allowed us to visualize internalization without permeabilizing the cells, thereby keeping the cells intact and not disrupting any membranes or endosomal compartments. According to the resulting confocal images, TacDAT co-localized only to a very limited degree with EGFP-Rab11 with distinct localization patterns for the M1 signal and the EGFP signal (Fig. 3*C*). For EGFP-Rab4, we observed dispersed co-localized vesicles, although the overall localization pattern appeared distinct from TacDAT (Fig. 3*C*). In contrast, we observed prominent co-localization for EGFP-Rab7 with multiple vesicular structures showing overlapping M1 and EGFP signals (Fig. 3*C*).

To assess whether constitutive internalization and postendocytic sorting were dependent on cell type, TacDAT was expressed in the dopaminergic cell line 1Rb3An27 (38). Similar to our observations in the HEK293 cells, TacDAT internalized constitutively, whereas no detectable constitutive internalization was observed in cells transfected with Tac (Fig. 4*A*). Because the 1Rb3An27 cells are difficult to transfect and because of poor cell adherence, we were not able to obtain a sufficiently high specific signal to carry out the ELISA internalization assay. Instead, we performed co-localization experiments like those carried out in the HEK293 cells. Similar to our observations in these cells, the confocal images indicated that TacDAT had the highest degree of co-localization with EGFP-Rab7 as supported by many co-localized vesicular structures (Fig. 4*B*). For EGFP-Rab4, we observed again dispersed co-localized vesicles, whereas co-localization with EGFP-Rab11 was poor (Fig. 4*B*). Quantification of the co-localization supported this with EGFP-Rab7 co-localization being significantly higher than the co-localization with EGFP-Rab11 (one-way ANOVA, $p < 0.01$, Bonferroni's

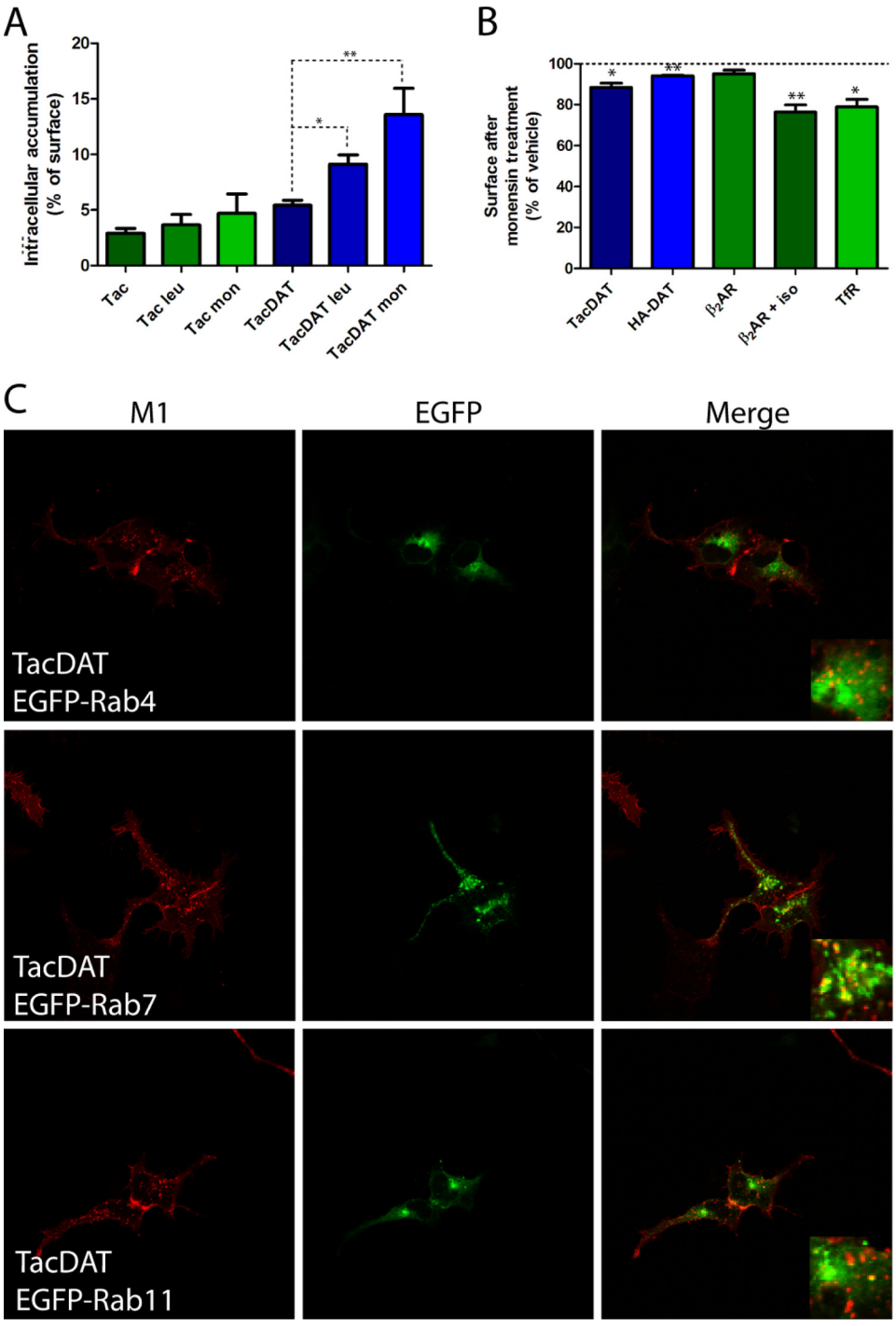

FIGURE 3. **Monensin and leupeptin affect DAT trafficking, and TacDAT co-localizes with late endosomal marker Rab7 in HEK293 cells.** *A*, intracellular accumulation measured by ELISA (described in Fig. 2*D*) in HEK293 cells transfected with Tac or TacDAT. The protease inhibitor leupeptin (*leu*) (100 μg/ml) or the recycling inhibitor monensin (*mon*) (25 μM) was included as indicated during the 1 h of internalization (means ± S.E. of $n = 4$; *, $p < 0.05$; **, $p < 0.01$; one-way ANOVA, Dunnett's multiple comparison test). *B*, surface expression determined in a surface ELISA of TacDAT, HA-DAT, control β_2-adrenergic receptor (β_2AR), isoproterenol (*iso*)-internalized β_2-adrenergic receptor, and EGFP-transferrin receptor (*TfR*) after 1-h treatment with monensin (25 μM) (means ± S.E. of $n = 3$–4; *, $p < 0.05$; **, $p < 0.01$; paired *t* test). *C*, confocal microscopy images of co-localization between TacDAT and EGFP-tagged Rab4, Rab7, and Rab11 after 1 h of Alexa Fluor 568-conjugated M1 antibody internalization in HEK293 cells. *Left panels* show Alexa Fluor 568 signal (*M1*), *middle panels* show EGFP signal, and *right panels* show the overlay of the two channels. Data are representative of at least three independent experiments.

multiple comparison test) and with intermediate EGFP-Rab4 co-localization (Fig. 4*D*). This suggests that constitutively internalized TacDAT is primarily sorted to a late endosomal pathway with some sorting also to an early endosome/short loop recycling pathway.

To verify that the sorting pattern observed for TacDAT was indeed a specific property of the transporter and not a pattern that would be seen for any membrane protein, we did parallel experiments in which we transiently expressed a FLAG-tagged β_2-adrenergic receptor in the 1Rb3An27 cells. The β_2-adrenergic receptor is internalized upon agonist treatment, and the internalized receptor is efficiently recycled (33, 34). In contrast to TacDAT, the β_2-adrenergic receptor transiently expressed in 1Rb3An27 cells did not constitutively internalize to any detectable extent (data not shown); however, treatment of the cells with the agonist isoproterenol (10 μM) caused a marked time-dependent internalization (supplemental Fig. S1). Co-expression with the three EGFP-Rab proteins showed for the internalized receptor a pattern markedly different from that seen for internalized TacDAT. In the confocal images, the M1 antibody signal overlapped quite prominently with the signal from both EGFP-Rab4 and EGFP-Rab11, whereas rather little overlap was seen with the signal from EGFP-Rab7 (Fig. 4*D*). Quantification of the signals confirmed this by showing significantly higher co-localization of the internalized β_2-adrenergic receptor with EGFP-Rab4 and EGFP-Rab11 than with EGFP-Rab7 (one-way ANOVA, $p < 0.001$, Bonferroni's multiple comparison test). This pattern of co-localization is consistent with postendocytic sorting of the β_2-adrenergic receptor to recycling pathways rather than to degradation. Note that the association of the β_2-adrenergic receptor with both the Rab4 pathway (39) and the Rab11 pathway (40) has been described previously.

To exclude that TacDAT displayed different postendocytic sorting as compared with DAT without Tac fused to the N terminus, we performed experiments in 1Rb3An27 cells on non-tagged DAT using our previously described rhodamine-coupled cocaine analogue JHC 1-64.

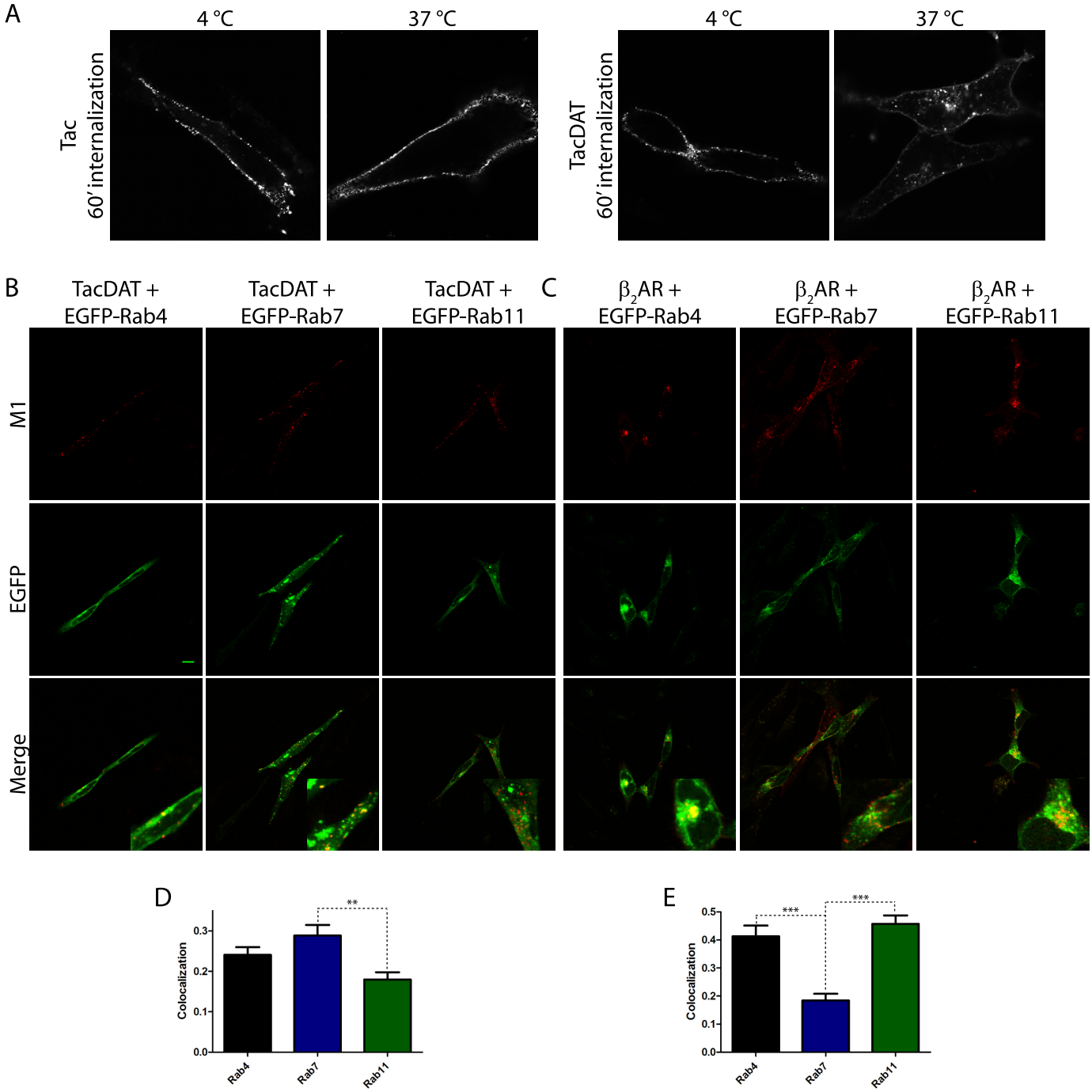

FIGURE 4. **TacDAT is constitutively internalized in the dopaminergic cell line 1Rb3An27 and co-localizes primarily with EGFP-Rab7 and intermediately with EGFP-Rab4.** *A*, experiment as in Fig. 2*A* on 1Rb3An27 cells expressing Tac or TacDAT. Pictures are representative of several experiments. *B*, fluorescence co-localization between TacDAT and the EGFP-tagged endosomal marker Rab4, Rab7, or Rab11 after 1 h of internalization in the presence of M1 antibody. *C*, fluorescence co-localization of FLAG-tagged β_2-adrenergic receptor (β_2AR), a *bona fide* recycling membrane protein, with EGFP-Rab4, -Rab7, or -Rab11 after 1 h of isoproterenol (10 μM)-induced internalization. In both *B* and *C*, *upper panels* show Alexa Fluor 568 signal (*M1*), *middle panels* EGFP signal, and *lower panels* show the overlay of the two channels. *D* and *E*, quantification of fluorescence co-localization in *B* and *C* between internalized TacDAT (*D*) or internalized FLAG-tagged β_2-adrenergic receptor (*E*) and the EGFP-tagged endosomal marker Rab4, Rab7, or Rab11 (means ± S.E., $p < 0.01$, one-way ANOVA, Bonferroni's multiple comparison test). Co-localization data were analyzed from 30 images of each condition. Representative images are shown in *B* and *C*.

This analogue enables fluorescent labeling of surface DAT in live cells with high specificity and was used recently to demonstrate constitutive internalization of endogenous DAT in dopaminergic neurons (8). Cells transiently co-expressing DAT and EGFP-tagged Rab4, Rab7, or Rab11 were labeled with JHC 1-64 and analyzed by confocal imaging after 1 h of internalization. Again we observed the most pronounced co-localization with EGFP-Rab7, less co-localization with EGFP-Rab4, and very limited co-localization with EGFP-Rab11 (Fig. 5). We also carried out time series experiments in the 1Rb3An27 cells expressing both DAT and EGFP-Rab7, showing that DAT-positive vesicles and EGFP-Rab7-positive vesi-

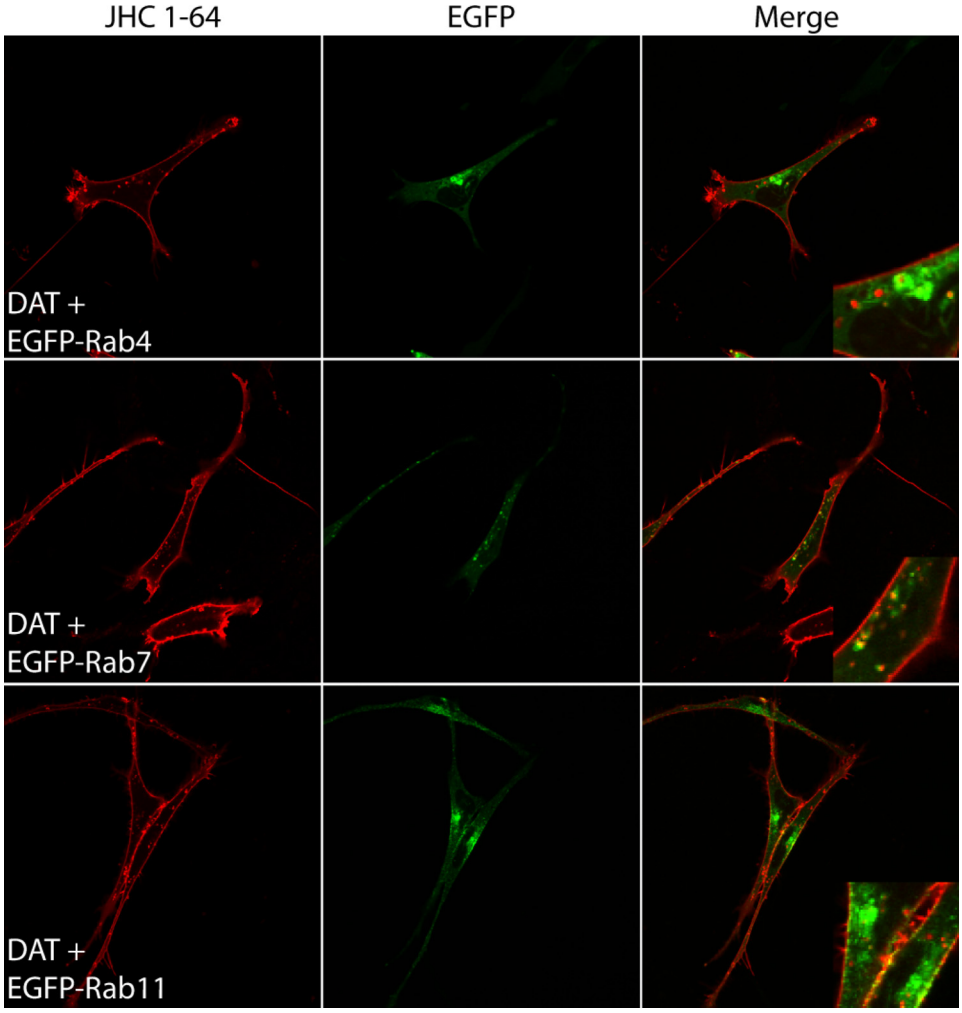

FIGURE 5. **Visualization of constitutive DAT internalization in live 1Rb3An27 cells using fluorescent cocaine analogue JHC 1-64 reveals predominant co-localization with EGFP-Rab7.** 1Rb3An27 cells expressing DAT together with EGFP-Rab4, -Rab7, or -Rab11 were incubated with JHC 1-64 (5 nM) at 4 °C to label surface DAT and subsequently incubated at 37 °C to drive internalization of DAT. After internalization, the live cells were imaged using confocal microscopy. *Left panels* show rhodamine signal (JHC 1-64), *middle panels* show EGFP signal, and *right panels* show the overlay of the two channels. Images are representative of three independent experiments.

cles were indeed identical as they co-migrated over time (supplemental Fig. S2).

To test whether endogenously expressed DAT exhibited the same postendocytic sorting pattern, we performed experiments in cultured rat midbrain dopaminergic neurons. As mentioned, we recently demonstrated a marked constitutive internalization of DAT in these neurons by labeling DAT with the fluorescent cocaine analogue JHC 1-64 (8). To determine the sorting of this constitutively internalized DAT, the dopaminergic cultures were transduced at 2–3 days *in vitro* with lentivirus encoding EGFP-Rab4, -Rab7, or -Rab11. After 10–14 days *in vitro*, the constitutive DAT internalization was analyzed using JHC 1-64 (1 h of internalization). As in the non-transduced neurons (8), we observed clear constitutive DAT internalization (Fig. 6*A*). The EGFP-tagged Rab proteins appeared to be expressed less well in the neurons; however, we were able to identify EGFP-positive vesicular structures in the cytoplasms of the somas and proximal extensions (Fig. 6*A*). As in the tested cell lines, the most evident co-localization was seen between EGFP-Rab7 and DAT/JHC 1-64 (Fig. 6*A*). We were also able to see DAT/JHC 1-64-positive vesicles overlapping with the signal from EGFP-Rab4, although this signal generally appeared rather diffuse. For EGFP-Rab11, the co-localization appeared very low (Fig. 6*A*). To further study whether the co-localization of DAT with the late endosomal marker Rab7 is a reflection of constitutively internalized DAT being sorted to a lysosomal degradation pathway, we looked at the constitutive DAT internalization in dopaminergic neurons together with the lysosomal marker LysoTracker Green. Substantial co-localization between internalized DAT and LysoTracker was observed (Fig. 6*B*), altogether supporting that constitutively internalized DAT most likely is sorted to a lysosomal degradative pathway with some possibly sorting also to a Rab4-positive short loop recycling pathway.

Previously, it has been suggested that ubiquitination of three lysines (Lys-19, Lys-27, and Lys-35) in the DAT N terminus drives the internalization observed in response to PMA (41). To assess whether this ubiquitination might play a role also in constitutive internalization as well as possibly in postendocytic sorting of the transporter, we generated an HA-DAT mutant in which the three lysines were mutated to arginines (HA-DAT 3KR). We chose to use the HA-DAT instead of TacDAT in these experiments to exclude any interference from tethering of the N terminus. Both HA-DAT and HA-DAT 3KR were expressed in 1RbAn27 cells, and constitutive internalization was determined using a double staining internalization assay (supplemental Fig. S3). According to the quantification, there was no significant difference between HA-DAT and HA-DAT 3KR, although there was a tendency to a lower internalization for HA-DAT 3KR (supplemental Fig. S3). This suggests that most of the constitutive internalization observed does not depend on ubiquitination of the DAT N terminus. To compare the sorting of the constitutively internalized HA-DAT and HA-DAT 3KR, we co-expressed the transporters together with EGFP-Rab4, -Rab7, and -Rab11. Similar to TacDAT, we observed that HA-DAT primarily co-localized with vesicular structures positive for EGFP-Rab7, whereas there appeared to be less co-localization with EGFP-Rab4 and EGFP-Rab11 (Fig. 7). The same co-localization pattern was observed for HA-DAT 3KR (Fig. 7). Altogether, these data suggest that neither constitutive internalization of DAT nor the subsequent postendocytic sorting depends on ubiquitination of the N terminus.

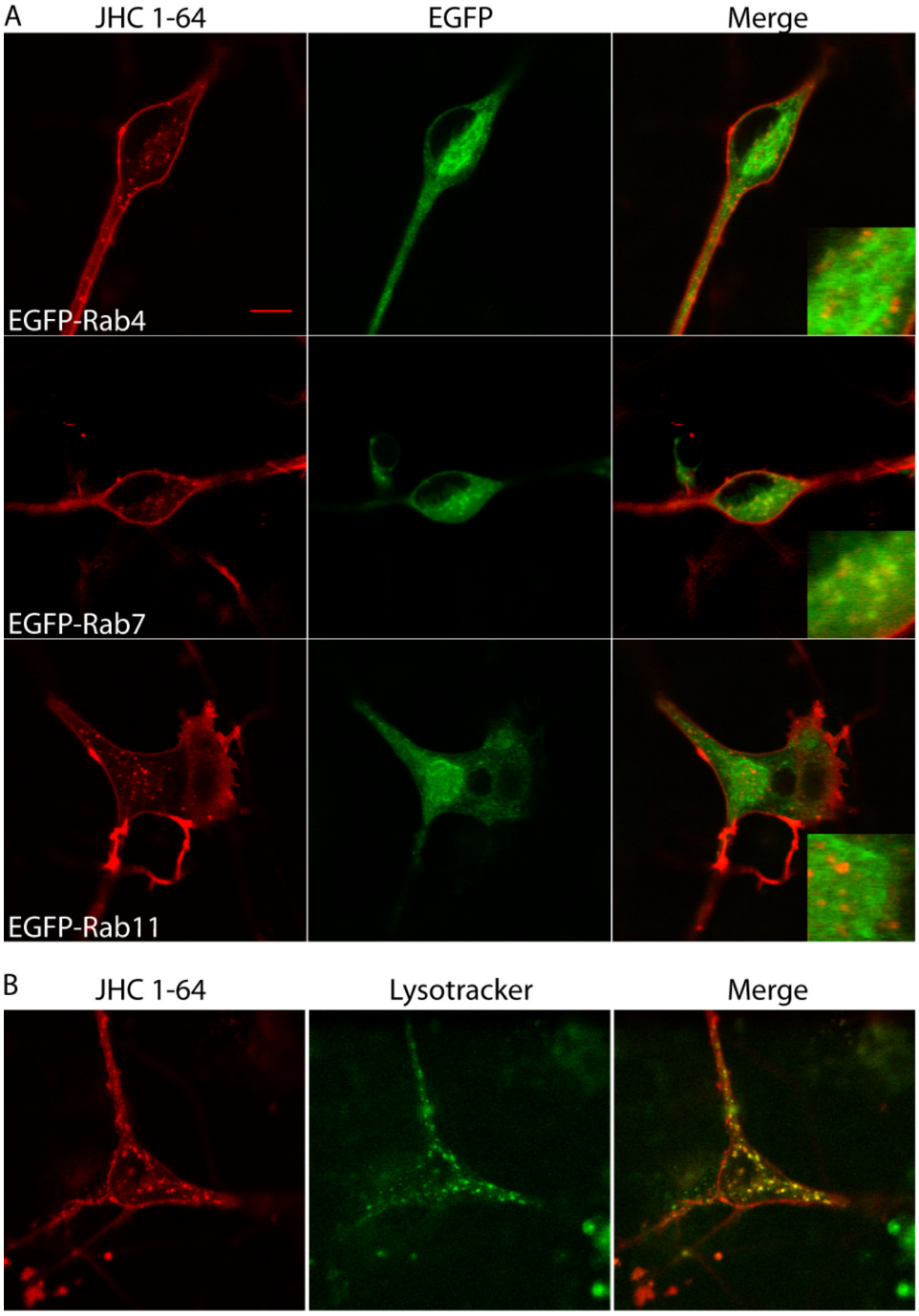

FIGURE 6. **Constitutive DAT internalization in cultured dopaminergic neurons is sorted to late endosomal/lysosomal pathway.** *A*, postnatal mesencephalic primary cultures from rat pups were transduced with lentivirus encoding EGFP-Rab4, -Rab7, or -Rab11 at days 2–3 *in vitro*. At days 10–14 *in vitro*, the cultures were used for constitutive DAT sorting experiments by incubating the cultures with 5 nM JHC 1-64 at 4 °C to label surface DAT before the cells were incubated at 37 °C for 1 h to drive the constitutive internalization. Subsequently, the live cells were imaged at room temperature using confocal microscopy. *Left panels* show rhodamine signal (*JHC 1-64*), *middle panels* show EGFP signal, and *right panels* show the overlay of the two channels. *B*, an experiment parallel to that in *A* was performed in non-transduced dopaminergic neurons where LysoTracker Green (100 nM) was added during the last 10 min of incubation before imaging. *Left*, JHC 1-64; *middle*, LysoTracker Green; *right*, overlay. Images are representative of at least three batches of neuronal cultures.

DISCUSSION

It is well established that DAT undergoes constitutive endocytosis in transfected heterologous cells (6, 10, 17), and recently it was demonstrated that also DAT endogenously expressed in dopaminergic neurons is constitutively internalized (8). However, the postendocytic sorting and fate of the internalized transporter have remained uncertain. In the current study, we addressed this question in both cell lines and dopaminergic neurons using a series of different complementary approaches.

DAT sorting was first studied using a new DAT fusion protein with an extra transmembrane segment. This TacDAT construct was made by fusing the single transmembrane protein Tac to DAT. Tac itself seems to be rather inert in its trafficking properties, and several studies have used Tac fusion proteins to define trafficking signals in cytosolic domains of membrane proteins including DAT (18) and other transporters (42, 43). Importantly, TacDAT displayed functional properties that overall were similar to DAT (Fig. 1*C*). Furthermore and in agreement with previously published data for DAT (6, 8–10, 44, 45), TacDAT was constitutively internalized, and it was internalized in response to PMA and amphetamine stimuli (Fig. 2, *C* and *E*). The observed trafficking properties for TacDAT are thus likely related to the DAT part of TacDAT because Tac alone, in agreement with previous observations (18), did not internalize to any detectable degree, neither constitutively nor in response to PMA (Fig. 2*C* and *E*).

Antibodies recognizing extracellular epitopes in membrane proteins are highly desirable for dynamic studies of their trafficking properties; however, it has proven notoriously difficult to develop an efficient antibody against an endogenous extracellular epitope of the DAT, and it has been difficult to introduce extracellular antibody tags in the extracellular domains of the transporter. Nevertheless, Sorkin and co-workers (22) were capable of introducing an HA tag in the large second extracellular loop (ECL2) and maintain transport activity and wild type expression upon transfection. Use of the epitope has already allowed interesting new insight into DAT trafficking using both heterologous cells and transfected

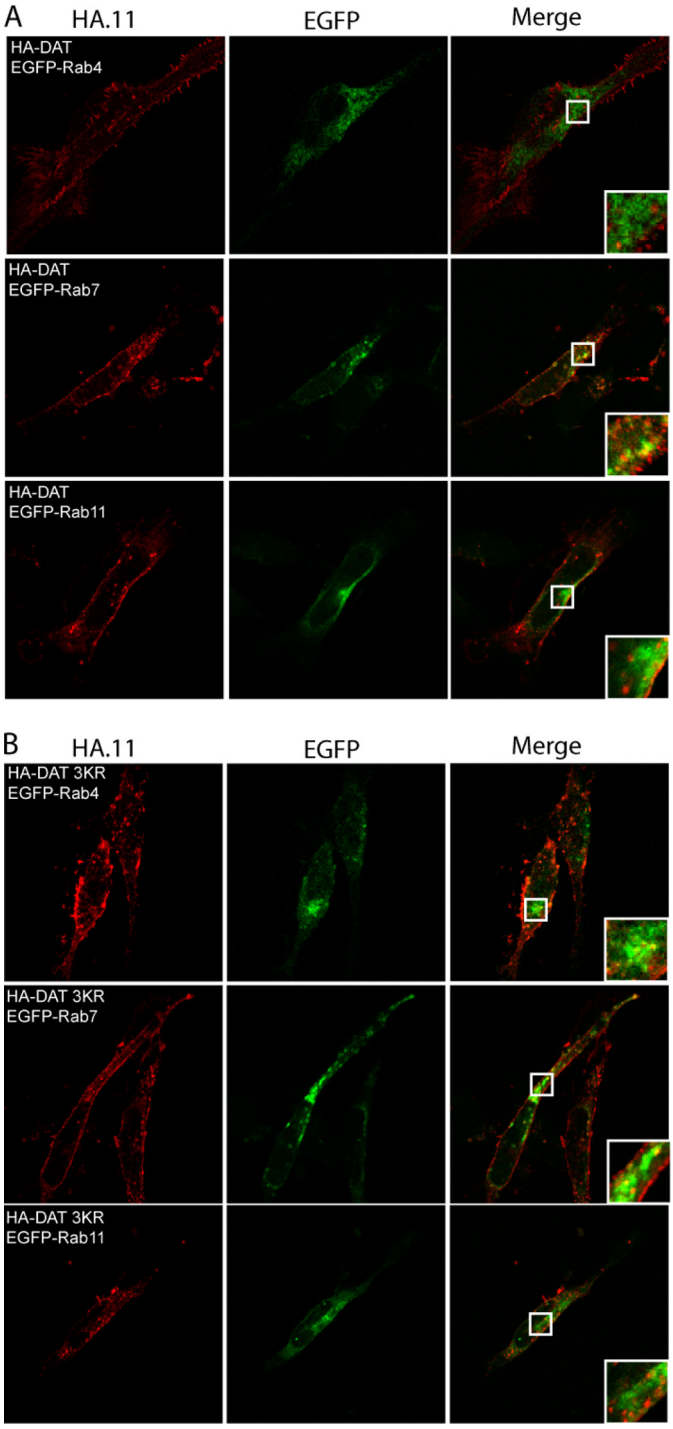

FIGURE 7. **Sorting of constitutively internalized HA-DAT does not depend on N-terminal ubiquitination.** 1Rb3An27 cells were transiently transfected with either HA-DAT (*A*) or a mutant (*B*) in which three main sites for ubiquitination (Lys-19, Lys-27, and Lys-35) were mutated to arginines (HA-DAT 3KR) and EGFP-Rab4, -Rab7, or -Rab11. The cells were surface-labeled with HA.11, and then internalization was driven for 1 h at 37 °C before staining and fixation. *Left panels* show Alexa Fluor 568 signal (*HA.11*), *middle panels* show EGFP signal, and *right panels* show the overlay of the two channels. The images shown are representative of at least two independent experiments.

dopaminergic neurons in culture (19, 22, 41). The present TacDAT construct represents an alternative way of generating an extracellular antibody epitope and carries several properties that complement already existing approaches for studying DAT trafficking. The M1 FLAG antibody epitope at the Tac N terminus harbors several desirable features. 1) It is outside the DAT primary sequence and thus unlikely to interfere with DAT function. 2) The M1 antibody bound to the FLAG epitope displays an almost 10 times higher signal per DAT molecule than the HA.11 antibody on the HA epitope in extracellular loop 2 (Fig. 1*E*). 3) The M1 antibody can be stripped off from the FLAG epitope, which is essential for the quantitative ELISA internalization assays (Fig. 2*E*) and not possible for the HA.11 antibody bound to HA-DAT (22). 4) Labeling of the FLAG epitope with M1 antibody can be done at 4 °C and thus at a truly trafficking-restricted temperature. This is not the case for labeling of HA-DAT with HA.11, which is only possible at 18 °C or higher (22). Furthermore, it interesting to consider extending the use of Tac fusion constructs to other transporters in the family. Importantly, fusing SERT and Tac head to tail results in a TacSERT construct that upon expression in HEK293 cells retains the trafficking properties of wild type SERT.[4] Thus, it might be possible to use Tac fusion constructs as a general means of tagging transporters, thereby allowing direct comparisons of trafficking properties between different transporters as well as dissection of distinct trafficking signals. We should note, however, that even though uptake and trafficking properties are preserved in Tac fusion constructs tethering of the N terminus might influence other less apparent functions; *e.g.* TacSERT was found to display impaired reverse transport (46). This does not preclude the use of Tac fusion constructs in trafficking studies but underlines that although the constructs might be advantageous observations should be supported by alternative strategies as also done in the present study.

Using a quantitative ELISA-based internalization assay in HEK293 cells expressing TacDAT, we showed that the apparent constitutive intracellular accumulation of TacDAT was increased by both inhibitor of lysosomal proteases (leupeptin) and the recycling/degradation inhibitor monensin (Fig. 3*A*). Monensin is a cationophore believed to exert its role on membrane protein trafficking by dissipating the pH gradient across the intracellular membranes, thereby bringing trafficking between intracellular compartments to a hold as this is dependent on differences in pH gradients (32). The apparent increase in intracellular accumulation in response to monensin might accordingly be an effect of both inhibiting sorting to lysosomal degradation and inhibiting recycling back to the plasma membrane. According to the surface ELISA, monensin reduced both TacDAT and HA-DAT surface expression, suggesting a detectable DAT recycling although to a lesser degree than what was observed for both the β_2-adrenergic receptor and the transferrin receptor (Fig. 3*B*). In another study using transfected porcine aortic endothelial cells, DAT surface expression and function were also reduced by monensin as assessed by surface biotinylation and dopamine uptake experiments (10). Regarding the uptake experiments, it is a caveat, however, as also noted by the authors that monensin as a sodium ionophore most likely would affect the sodium plasma membrane sodium gradient, which is the driving

[4] T. N. Jørgensen and U. Gether, unpublished observations.

force for dopamine transport; *i.e.* a reduction in dopamine uptake in response to monensin cannot necessarily be attributed to reduced surface expression (10).

In our further strategy to investigate DAT postendocytic sorting, we used Rab proteins fused to EGFP in combination with confocal imaging. The EGFP-tagged Rab proteins were distributed in the cells as would be expected according to the vesicular compartments that they label with a perinuclear vesicular pattern for Rab4 (early endosomes/recycling) (47, 48), a pericentriolar localization for Rab11 (long loop recycling) (48), and a large sized vesicular pattern for Rab7 (late endosomes) (49) (see Figs. 2–6). In HEK293 cells, co-expression of TacDAT with the EGFP-tagged Rab proteins showed the most pronounced co-localization with the late endosomal marker Rab7 (Fig. 3*C*) and less co-localization with Rab4 and Rab11. Similarly, in the dopaminergic cell line 1Rb3An27, we observed clear constitutive internalization, and when probing the co-localization with the EGFP-tagged Rab proteins in a quantitative manner, the highest co-localization was observed with Rab7, which was significantly higher than with Rab11 but not Rab4, which displayed an intermediate co-localization with TacDAT (Fig. 4*D*). The sorting pattern observed was most likely not an artifact of the assay because only cells expressing TacDAT internalized M1 antibody (data not shown). In addition, parallel experiments in the 1Rb3An27 cells with the β_2-adrenergic receptor exhibited a different co-localization pattern characterized by highest co-localization with Rab4 and Rab11 (Fig. 4*E*) as expected for proteins well known to undergo efficient recycling. This observation, based on the use of the exact same antibody epitope and antibody, strongly supports that the quantification does indeed reflect properties of the analyzed protein. Furthermore, we observed the same co-localization pattern as for TacDAT when using our previously described fluorescent cocaine analogue JHC 1-64 as a label to follow postendocytic sorting of non-tagged DAT. Finally, we studied sorting of the internalized endogenous DAT in dopaminergic primary cultures that were transduced with lentivirus encoding EGFP-tagged Rab4, Rab7, or Rab11. Constitutive internalization of endogenous DAT was visualized using the cocaine analogue JHC 1-64, and we observed a sorting pattern similar to that observed in the cell lines (Fig. 6*A*). Additionally, we observed a profound co-localization between DAT and lysosomal marker LysoTracker, further supporting that constitutively internalized DAT is sorted to late endosome/degradation in dopaminergic neurons (Fig. 6*B*).

Previous reports have proposed that constitutively internalized DAT is sorted to a recycling pathway (10, 17, 50). The present data are in agreement with a detectable recycling of DAT as we observed a reduction of TacDAT and HA-DAT surface expression upon monensin treatment (Fig. 3*B*) and an intermediate co-localization of constitutively internalized DAT with EGFP-Rab4. Of note, DAT was suggested to undergo fast constitutive recycling in transfected PC12 cells (17), which also might be in agreement with our observation that DAT exhibited some co-localization with Rab4. In a recent study, it was proposed that DAT is recycled via a Rab11-dependent pathway because the level of DAT in the plasma membrane was increased upon co-expression of constitutively active Rab11, but all experiments were steady state experiments, and a dominant negative Rab11 mutant did not exhibit any effect compared with a GFP control when quantifying DAT surface binding (50). Moreover, Rab11 has been shown to be important for Golgi to plasma membrane trafficking (51), thus affecting the plasma membrane targeting of newly synthesized protein. Other transporters in the neurotransmitter-sodium symporter family, however, might associate with a Rab11-dependent pathway; *e.g.* the neuronal glycine transporter GlyT2 co-localized significantly with Rab11, and a dominant negative Rab11 mutant affected GlyT2 subcellular distribution (52). Of note, we did not observe any redistribution of DAT upon co-expression with the dominant negative Rab11 mutant (data not shown).

It has been demonstrated that ubiquitination of three lysines in the DAT N terminus is critical for mediating PMA-induced internalization of DAT (41). Interestingly, lysyl ubiquitination is also well known to operate as a signal critical for lysosomal sorting of endocytosed integral membrane proteins including certain G protein-coupled receptors (53–55). One example is the CXCR4 chemokine receptor in which mutational disruption of lysyl ubiquitination blocks trafficking of the receptor to lysosomes and leads to recycling rather than lysosomal degradation (56–58) Our observations show a clearly different pattern for DAT; *i.e.* neither constitutive internalization nor postendocytic sorting is dependent on N-terminal lysyl ubiquitination of DAT. Notably, a similar non-ubiquitin-dependent sorting to lysosomal degradation has been described for the δ-opioid receptor (59) even though the receptor is also readily ubiquitinated (60).

In summary, our data suggest that constitutively internalized DAT is sorted to late endosomes/lysosomes as well as in part to recycling through a short loop recycling pathway. The fact that the sorting pattern is the same in three different cellular systems (HEK293 cells, 1Rb3An27 cells, and cultured dopaminergic neurons) suggests that the constitutive internalization depends on general cellular factors as opposed to the PKC-mediated DAT internalization for which the cellular environment seems to affect the PKC stimulation to a high degree (8, 61). The sorting of DAT to both degradation and recycling suggests a potential for DAT to be directed to different pathways upon internalization. In the future, it should be highly interesting to investigate to what degree postendocytic sorting might be subject to regulation and redirection by yet unknown mechanisms with putative impact on the overall regulation of dopaminergic signaling.

Acknowledgments—We thank Dr. Mark von Zastrow for the pcDNA3.1 FLAG-β_2-adrenergic receptor plasmid, Dr. Bo van Deurs for the pJPA5 transferrin receptor-GFP plasmid, Dr. José A. Esteban for the pEGFP-Rab4 plasmid, and Dr. Katherine W. Roche for pEGFP-Rab7 and pEGFP-Rab11 plasmids. We thank Anette Dencker Kristensen and Nabeela Khadim for excellent technical assistance and Dr. Mu-Fa Zou for synthesizing the JHC 1-64 batch.

REFERENCES

1. Chen, N. H., Reith, M. E., and Quick, M. W. (2004) *Pflugers Arch.* **447,** 519–531
2. Gether, U., Andersen, P. H., Larsson, O. M., and Schousboe, A. (2006) *Trends Pharmacol. Sci.* **27,** 375–383
3. Torres, G. E., and Amara, S. G. (2007) *Curr. Opin. Neurobiol.* **17,** 304–312
4. Gainetdinov, R. R., and Caron, M. G. (2003) *Annu. Rev. Pharmacol. Toxicol.* **43,** 261–284
5. Torres, G. E., Gainetdinov, R. R., and Caron, M. G. (2003) *Nat. Rev. Neurosci.* **4,** 13–25
6. Chi, L., and Reith, M. E. (2003) *J. Pharmacol. Exp. Ther.* **307,** 729–736
7. Daniels, G. M., and Amara, S. G. (1999) *J. Biol. Chem.* **274,** 35794–35801
8. Eriksen, J., Rasmussen, S. G., Rasmussen, T. N., Vaegter, C. B., Cha, J. H., Zou, M. F., Newman, A. H., and Gether, U. (2009) *J. Neurosci.* **29,** 6794–6808
9. Melikian, H. E., and Buckley, K. M. (1999) *J. Neurosci.* **19,** 7699–7710
10. Sorkina, T., Hoover, B. R., Zahniser, N. R., and Sorkin, A. (2005) *Traffic* **6,** 157–170
11. Zhu, S. J., Kavanaugh, M. P., Sonders, M. S., Amara, S. G., and Zahniser, N. R. (1997) *J. Pharmacol. Exp. Ther.* **282,** 1358–1365
12. Copeland, B. J., Vogelsberg, V., Neff, N. H., and Hadjiconstantinou, M. (1996) *J. Pharmacol. Exp. Ther.* **277,** 1527–1532
13. Vaughan, R. A., Huff, R. A., Uhl, G. R., and Kuhar, M. J. (1997) *J. Biol. Chem.* **272,** 15541–15546
14. Garcia, B. G., Wei, Y., Moron, J. A., Lin, R. Z., Javitch, J. A., and Galli, A. (2005) *Mol. Pharmacol.* **68,** 102–109
15. Morón, J. A., Zakharova, I., Ferrer, J. V., Merrill, G. A., Hope, B., Lafer, E. M., Lin, Z. C., Wang, J. B., Javitch, J. A., Galli, A., and Shippenberg, T. S. (2003) *J. Neurosci.* **23,** 8480–8488
16. Zahniser, N. R., and Sorkin, A. (2009) *Semin. Cell Dev. Biol.* **20,** 411–417
17. Loder, M. K., and Melikian, H. E. (2003) *J. Biol. Chem.* **278,** 22168–22174
18. Holton, K. L., Loder, M. K., and Melikian, H. E. (2005) *Nat. Neurosci.* **8,** 881–888
19. Sorkina, T., Richards, T. L., Rao, A., Zahniser, N. R., and Sorkin, A. (2009) *J. Neurosci.* **29,** 1361–1374
20. Madsen, K. L., Eriksen, J., Milan-Lobo, L., Han, D. S., Niv, M. Y., Ammendrup-Johnsen, I., Henriksen, U., Bhatia, V. K., Stamou, D., Sitte, H. H., McMahon, H. T., Weinstein, H., and Gether, U. (2008) *Traffic* **9,** 1327–1343
21. Loland, C. J., Gråsäs, C., Javitch, J. A., and Gether, U. (2004) *J. Biol. Chem.* **279,** 3228–3238
22. Sorkina, T., Miranda, M., Dionne, K. R., Hoover, B. R., Zahniser, N. R., and Sorkin, A. (2006) *J. Neurosci.* **26,** 8195–8205
23. Rayport, S., Sulzer, D., Shi, W. X., Sawasdikosol, S., Monaco, J., Batson, D., and Rajendran, G. (1992) *J. Neurosci.* **12,** 4264–4280
24. di Porzio, U., Daguet, M. C., Glowinski, J., and Prochiantz, A. (1980) *Nature* **288,** 370–373
25. Naldini, L., Blömer, U., Gallay, P., Ory, D., Mulligan, R., Gage, F. H., Verma, I. M., and Trono, D. (1996) *Science* **272,** 263–267
26. Loland, C. J., Norregaard, L., and Gether, U. (1999) *J. Biol. Chem.* **274,** 36928–36934
27. Chmelar, R. S., and Nathanson, N. M. (2006) *J. Biol. Chem.* **281,** 35381–35396
28. Cha, J. H., Zou, M. F., Adkins, E. M., Rasmussen, S. G., Loland, C. J., Schoenenberger, B., Gether, U., and Newman, A. H. (2005) *J. Med. Chem.* **48,** 7513–7516
29. Lavezzari, G., McCallum, J., Dewey, C. M., and Roche, K. W. (2004) *J. Neurosci.* **24,** 6383–6391
30. Lavezzari, G., and Roche, K. W. (2007) *Neuropharmacology* **52,** 100–107
31. Mu, Y., Otsuka, T., Horton, A. C., Scott, D. B., and Ehlers, M. D. (2003) *Neuron* **40,** 581–594
32. Mollenhauer, H. H., Morré, D. J., and Rowe, L. D. (1990) *Biochim. Biophys. Acta* **1031,** 225–246
33. Cong, M., Perry, S. J., Hu, L. A., Hanson, P. I., Claing, A., and Lefkowitz, R. J. (2001) *J. Biol. Chem.* **276,** 45145–45152
34. Gage, R. M., Kim, K. A., Cao, T. T., and von Zastrow, M. (2001) *J. Biol. Chem.* **276,** 44712–44720
35. Maxfield, F. R., and McGraw, T. E. (2004) *Nat. Rev. Mol. Cell Biol.* **5,** 121–132
36. Stenmark, H. (2009) *Nat. Rev. Mol. Cell Biol.* **10,** 513–525
37. Jones, M. C., Caswell, P. T., and Norman, J. C. (2006) *Curr. Opin. Cell Biol.* **18,** 549–557
38. Adams, F. S., La Rosa, F. G., Kumar, S., Edwards-Prasad, J., Kentroti, S., Vernadakis, A., Freed, C. R., and Prasad, K. N. (1996) *Neurochem. Res.* **21,** 619–627
39. Yudowski, G. A., Puthenveedu, M. A., Henry, A. G., and von Zastrow, M. (2009) *Mol. Biol. Cell* **20,** 2774–2784
40. Moore, R. H., Millman, E. E., Alpizar-Foster, E., Dai, W., and Knoll, B. J. (2004) *J. Cell Sci.* **117,** 3107–3117
41. Miranda, M., Dionne, K. R., Sorkina, T., and Sorkin, A. (2007) *Mol. Biol. Cell* **18,** 313–323
42. Kalandadze, A., Wu, Y., Fournier, K., and Robinson, M. B. (2004) *J. Neurosci.* **24,** 5183–5192
43. Colgan, L., Liu, H., Huang, S. Y., and Liu, Y. J. (2007) *Traffic* **8,** 512–522
44. Kahlig, K. M., Lute, B. J., Wei, Y., Loland, C. J., Gether, U., Javitch, J. A., and Galli, A. (2006) *Mol. Pharmacol.* **70,** 542–548
45. Sorkina, T., Doolen, S., Galperin, E., Zahniser, N. R., and Sorkin, A. (2003) *J. Biol. Chem.* **278,** 28274–28283
46. Sucic, S., Dallinger, S., Zdrazil, B., Weissensteiner, R., Jørgensen, T. N., Holy, M., Kudlacek, O., Seidel, S., Cha, J. H., Gether, U., Newman, A. H., Ecker, G. F., Freissmuth, M., and Sitte, H. H. (2010) *J. Biol. Chem.* **285,** 10924–10938
47. Daro, E., van der Sluijs, P., Galli, T., and Mellman, I. (1996) *Proc. Natl. Acad. Sci. U.S.A.* **93,** 9559–9564
48. Sönnichsen, B., De Renzis, S., Nielsen, E., Rietdorf, J., and Zerial, M. (2000) *J. Cell Biol.* **149,** 901–914
49. Bucci, C., Thomsen, P., Nicoziani, P., McCarthy, J., and van Deurs, B. (2000) *Mol. Biol. Cell* **11,** 467–480
50. Furman, C. A., Lo, C. B., Stokes, S., Esteban, J. A., and Gnegy, M. E. (2009) *Neurosci. Lett.* **463,** 78–81
51. Chen, W., Feng, Y., Chen, D., and Wandinger-Ness, A. (1998) *Mol. Biol. Cell* **9,** 3241–3257
52. Núñez, E., Pérez-Siles, G., Rodenstein, L., Alonso-Torres, P., Zafra, F., Jiménez, E., Aragón, C., and López-Corcuera, B. (2009) *Traffic* **10,** 829–843
53. Raiborg, C., Rusten, T. E., and Stenmark, H. (2003) *Curr. Opin. Cell Biol.* **15,** 446–455
54. Saksena, S., Sun, J., Chu, T., and Emr, S. D. (2007) *Trends Biochem. Sci* **32,** 561–573
55. Tsao, P. I., and von Zastrow, M. (2001) *Pharmacol. Ther.* **89,** 139–147
56. Bhandari, D., Trejo, J., Benovic, J. L., and Marchese, A. (2007) *J. Biol. Chem.* **282,** 36971–36979
57. Marchese, A., and Benovic, J. L. (2001) *J. Biol. Chem.* **276,** 45509–45512
58. Marchese, A., Raiborg, C., Santini, F., Keen, J. H., Stenmark, H., and Benovic, J. L. (2003) *Dev. Cell* **5,** 709–722
59. Tanowitz, M., and Von Zastrow, M. (2002) *J. Biol. Chem.* **277,** 50219–50222
60. Hislop, J. N., Henry, A. G., Marchese, A., and von Zastrow, M. (2009) *J. Biol. Chem.* **284,** 19361–19370
61. Mortensen, O. V., Larsen, M. B., Prasad, B. M., and Amara, S. G. (2008) *Mol. Biol. Cell* **19,** 2818–2829